

Rate-equation approach for a charge qudit

M. P. Liul,^{1,*} A. I. Ryzhov,^{1,2} and S. N. Shevchenko¹

¹*B. Verkin Institute for Low Temperature Physics and Engineering, Kharkiv 61103, Ukraine*

²*Quantum Computing Center, RIKEN, Wakoshi, Saitama 351-0198, Japan*

(Dated: April 11, 2023)

We theoretically describe the two-electron four-level double quantum dot (DQD) tunnel-coupled to a fermionic sea by using the rate-equation formalism. This approach allows to find occupation probabilities of each DQD level in a relatively simple way, compared to other methods. Calculated dependencies were compared with the experimental results. The system under study is irradiated by a strong driving signal and as a result one can observe Landau-Zener-Stückelberg-Majorana (LZSM) interferometry patterns which are successfully described by the considered formalism. The system operation regime depends on the amplitude of the excitation signal and the energy detuning, so one can transfer the system to the necessary quantum state in the most efficient way by setting these parameters. Obtained results give useful insights about initializing, characterizing and controlling the system quantum states.

I. INTRODUCTION

Fast developing of quantum computing field requires sophisticated practical solutions. One of such solutions are quantum dots. These systems are good candidates for being building blocs of quantum computers since they have good tunability [1] and flexible coupling geometry [2]. Also quantum dots demonstrate good performance for readout, manipulation and initialization of their spin states [3–6]. Such system can be used for quantum information [7, 8] and quantum computing [9,10]. Considered objects are also interesting for studying quantum luminescence [11, 12], superconductivity [13], Kondo effect [14], solid-state energy conversion [15], quantum communication [16,17] piezomagnetic effect [18], etc.

For solving many modern problems (one of them is a creation of a quantum computer) it is not enough to use a single quantum dot, thus one should connect them into chains [19]. The behaviour of electrons in a chain can be decomposed on interactions between pairs of adjacent dots, called double quantum dots (DQD). As a result these systems are widely explored nowadays, particularly, it was stressed that DQDs open opportunities for probing electron-phonon coupling [20], allow to probe the semiconductor environment [21], can be used in the relatively new and promising area of spintronics [22], serve as thermoelectric generators [23] and noise detectors [24]. So both experimental and theoretical study of such systems is very important not only from quantum information point of view but also for modern quantum physics in general.

In the current paper we theoretically study the properties of a qudit (d -level quantum system) [25–27] experimentally studied in Ref. [28]. The main tool of our analysis is the rate-equation formalism [29–31], which is relatively simple, but often shows good agreement with experiments. For example, this method successfully describes the behaviour of a two-level system [32] as well as a multi-level system (solid-state artificial atom) from Ref. [33] which was analyzed in Ref. [34].

The presented research also could be interesting since it opens an additional opportunity for studying the Landau-Zener-Stückelberg-Majorana (LZSM) transitions. This effect can be observed if one irradiates a quantum system by a signal with the frequency which is much smaller than the distance between energy levels [35]. LZSM transitions are reflected in many fields, for instance, in solid-state physics [36,37], quantum information science [38,39], nuclear physics [40], chemical physics [41], quantum optics [42]. Repeated LZSM transitions result in LZSM interference [43–47]. The LZSM interferometry can be used for a quantum system description and control [48,49], it allows to understand better processes of photon-assisted transport in superconducting systems [50] and decoherence in quantum systems [51,52].

The rest of the paper is organized as follows. In Sec. II the rate-equation formalism for a TLS is laid out with its following expansion on multi-level systems. The considered model was applied for the analysis of the two-electron double quantum dot in Sec. III. Sec. IV is devoted to a DQD studied in the three-level approximation. In Sec. V we present our conclusions. The expressions for building DQD energy levels diagram were obtained in Appendix A.

II. RATE-EQUATION APPROACH

In this section we describe theoretical aspects of the rate-equation formalism. For doing this we firstly employ this method for a two-level system with further extension of obtained results on multi-level systems. The Hamiltonian of

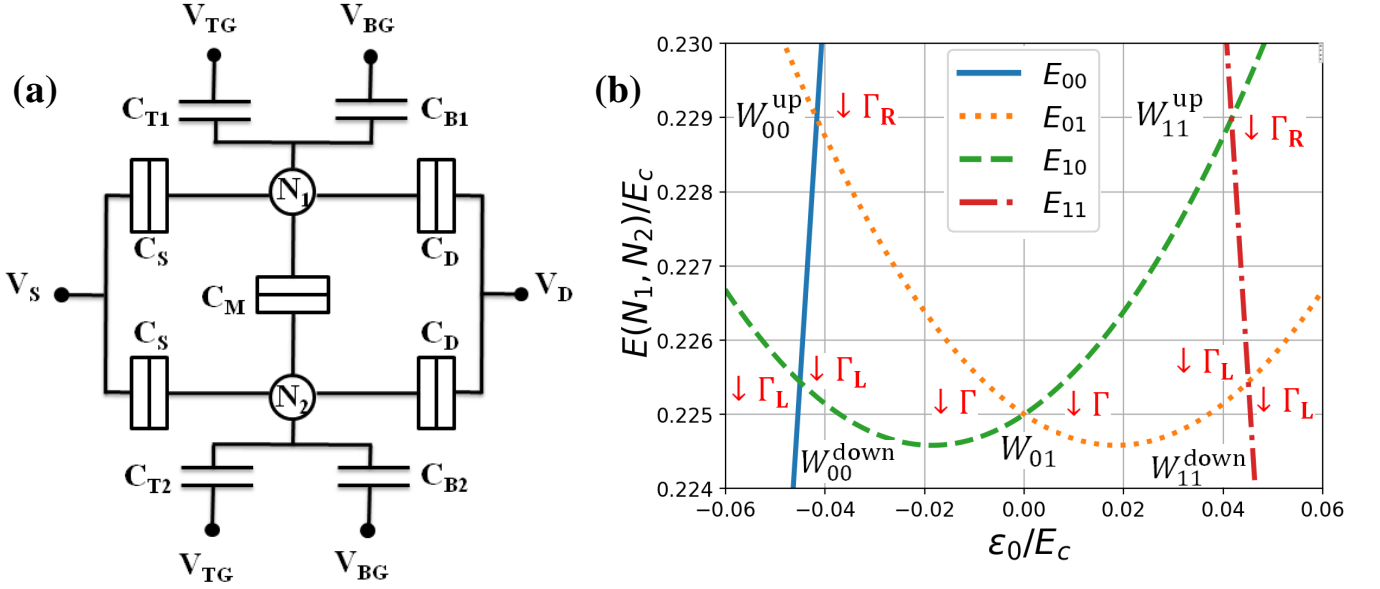


Figure 1: Scheme of the DQD and its energy levels. Panel (a) shows the electrical scheme of the considered DQD, with N_1 and N_2 being the number of electrons in each dot, V and C with the corresponding subscripts indicate the applied voltages and capacitances respectively. (b) Energy levels of the DQD studied in Ref. [28], where $W_{00(11)}^{\text{up}}$, $W_{00(11)}^{\text{down}}$ are the transition rates between the state $|00\rangle$ ($|11\rangle$) and states $|01\rangle$, $|10\rangle$ ($|10\rangle$, $|01\rangle$) respectively; W_{01} is a transition rate between states $|01\rangle$ and $|10\rangle$, Δ with the same subscript indicates the corresponding tunnel coupling, $\Gamma_{L(R)}$ is the relaxation rate between left (right) dot and reservoirs, Γ is the relaxation rate between states $|01\rangle$ and $|10\rangle$.

a TLS, driven by external field can be written in the form:

$$\hat{H}(t) = -\frac{\Delta}{2}\hat{\sigma}_x - \frac{h(t)}{2}\hat{\sigma}_z, \quad (1)$$

where $\hat{\sigma}_z = \begin{pmatrix} 1 & 0 \\ 0 & -1 \end{pmatrix}$ and $\hat{\sigma}_x = \begin{pmatrix} 0 & 1 \\ 1 & 0 \end{pmatrix}$ are Pauli matrices, Δ is the level splitting, $h(t)$ is the external excitation which can be presented as follows:

$$h(t) = \varepsilon + A \sin 2\pi\nu t + \delta\varepsilon_{\text{noise}}(t). \quad (2)$$

Here ε is an energy detuning, ν and A are the frequency of the excitation field and its amplitude respectively, $\delta\varepsilon_{\text{noise}}(t)$ can be treated as the classical noise. In Ref. [32] the authors used the white-noise model and for the LZSM transition rate they obtained (see also Refs. [53–57])

$$W(\varepsilon, A) = \frac{\Delta^2}{2} \sum_n \frac{\Gamma_2 J_n^2(A/\nu)}{(\varepsilon - n\nu)^2 + \Gamma_2^2}. \quad (3)$$

Here Γ_2 is the decoherence rate, J_n is the Bessel function, and the reduced Planck constant is equal to unity ($\hbar = 1$). Equation (3) characterizes the transitions which happen when a system passes through a point of maximum levels approaching.

In the case of a multi-level system we should assign a corresponding transition rate to each level quasicrossing point (point of maximum levels approaching). The authors of Ref. [34] proposed to extend Eq. (3) on the transition between arbitrary states $|i\rangle$ and $|j\rangle$ of a multi-level system by the formula:

$$W_{ij}(\varepsilon_{ij}, A) = \frac{\Delta_{ij}^2}{2} \sum_n \frac{\Gamma_2 J_n^2(A/\nu)}{(\varepsilon_{ij} - n\nu)^2 + \Gamma_2^2}, \quad (4)$$

where Δ_{ij} is the energy splitting between states $|i\rangle$ and $|j\rangle$, ε_{ij} is the corresponding energy detuning. Then the rate equation for the $|i\rangle$ state can be expressed

$$\frac{dP_i}{dt} = \sum_j W_{ij}(P_j - P_i) + \sum_{i'} \Gamma_{i'i} P_{i'} - \sum_{i'} \Gamma_{ii'} P_i. \quad (5)$$

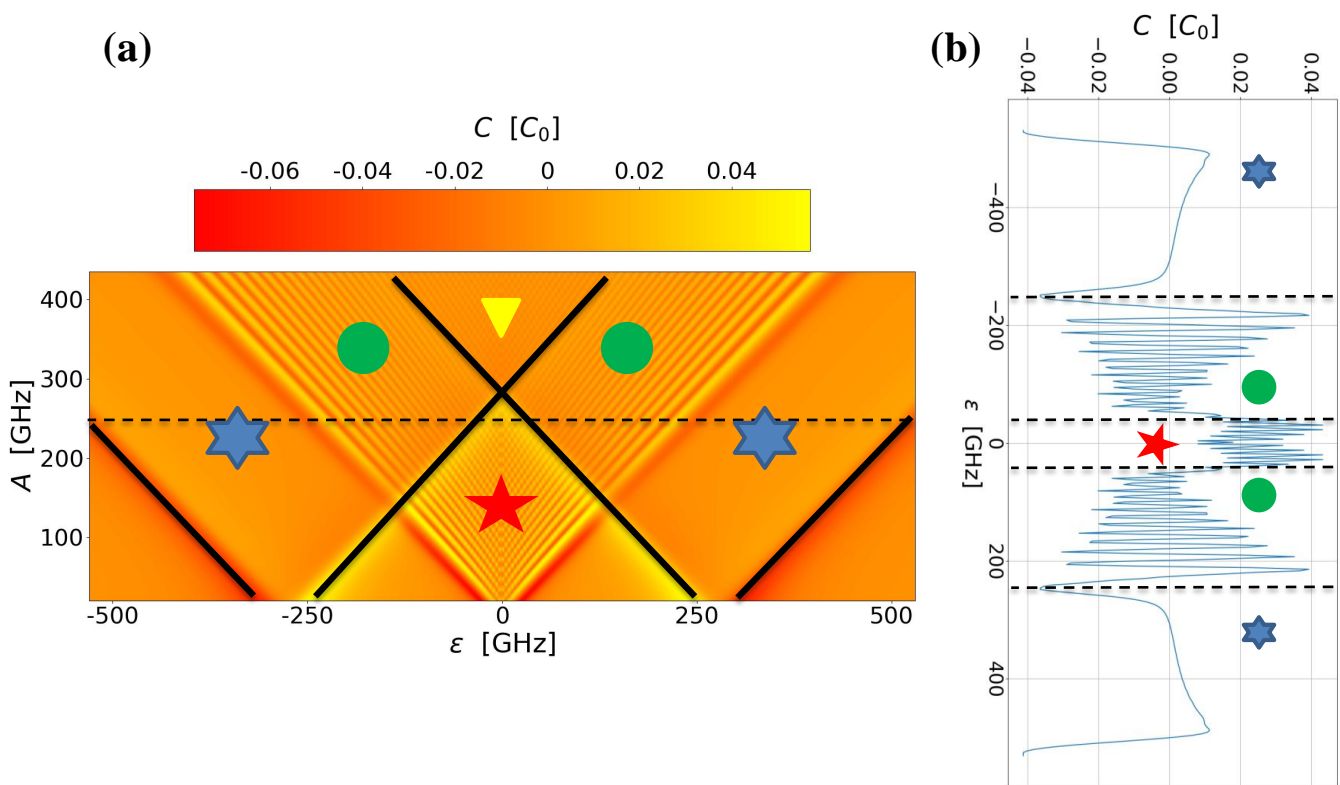


Figure 2: (a) Parametric capacitance of the DQD as a function of the excitation field amplitude A and the energy detuning ε . (b) Dependence of the parametric capacitance of the DQD on the energy detuning ε for the excitation field amplitude $A = 240$ GHz (a line cut of panel (a) along y -axis). The corresponding relaxation rates of the system are $\Gamma_1 = 0.9$ GHz, $\Gamma_R = 12$ GHz, $\Gamma_L = 50$ MHz. The energy splittings are equal to $\Delta_c = 8.25$ GHz, $\Delta_{\text{up}} = 1$ GHz, $\Delta_{\text{down}} = 21$ GHz, and their positions are at $\varepsilon = 0, \pm 255$ and ± 276 GHz respectively. The decoherence rate $\Gamma_2 = 4$ GHz and the excitation frequency $\nu = 4$ GHz.

Here P_i is the probability that a system occupies $|i\rangle$ state, $\Gamma_{ii'}$ characterize the relaxation from the state $|i\rangle$ to the state $|i'\rangle$.

Thus, writing equations (5) for each level we can find occupation probabilities of the levels and then build corresponding interferograms. Usually for simplicity one considers only a stationary case, $dP_i/dt = 0$. The solution of such a system will not describe a quantum object dynamics, but it is suitable for obtaining its main properties. Also we can use the fact that the sum of all probabilities is equal to unity $\sum_i P_i = 1$.

III. RATE EQUATIONS AND INTERFEROGRAM FOR THE DQD

In this section we apply the rate-equation formalism to the parallel DQD. The scheme of the considered system is depicted in Fig. 1(a), where N_1, N_2 are numbers of electrons in each dot, V and C with the corresponding subscripts indicate the applied voltages and capacitances respectively. Figure 1(b) shows the energy levels diagram. The detailed procedure of an energy levels diagram building from the scheme in Fig. 1(a) is described in Appendix A.

Since we consider charge states of the system and after each point of maximum levels approaching corresponding levels swap their positions (an upper level becomes a lower one and vice versa), and we should take this fact into account. Especially this effect will have an influence on relaxations which occur from the upper level to the lower one. We imply that inverse relaxations are Boltzmann suppressed. To handle this we separate our interval into two parts: for the first interval $\varepsilon < 0$ and for the second interval $\varepsilon \geq 0$. Also it is important to mention that in our calculations (not shown here) we divided our picture into more parts (6 is the maximum), but it had worse performance. So finally, for the considered case the rate equations (5) take the form

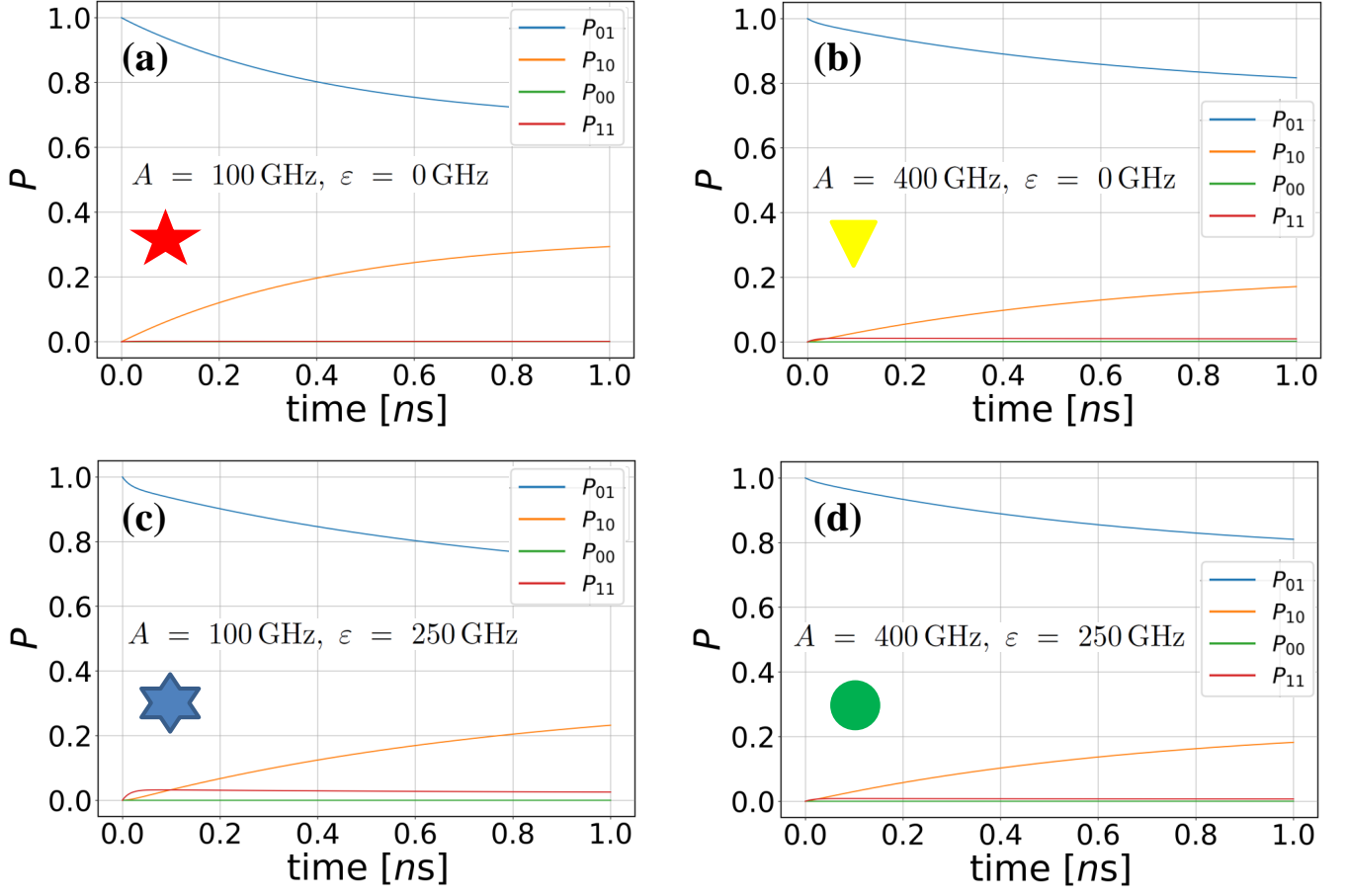


Figure 3: Time dependence of probabilities for different regimes: (a) multi-passage LZSM; (b) single-passage LZSM; (c) incoherent LZSM; (d) double-passage LZSM. The parameters are the same with Fig. 2.

Interval I ($\varepsilon < 0$):

$$\begin{cases} \dot{P}_{01} = W_{10}(P_{10} - P_{01}) + W_{11}^{\text{down}}(P_{11} - P_{01}) + W_{00}^{\text{up}}(P_{00} - P_{01}) - \Gamma P_{01} + \Gamma_R P_{00} + \Gamma_L P_{11} \\ \dot{P}_{10} = W_{11}^{\text{up}}(P_{11} - P_{10}) + W_{00}^{\text{down}}(P_{00} - P_{10}) + W_{10}(P_{01} - P_{10}) + \Gamma P_{01} + \Gamma_L P_{00} + \Gamma_R P_{11} \\ \dot{P}_{00} = W_{00}^{\text{down}}(P_{10} - P_{00}) + W_{00}^{\text{up}}(P_{01} - P_{00}) - \Gamma_R P_{00} - \Gamma_L P_{00} \\ P_{01} + P_{10} + P_{00} + P_{11} = 1 \end{cases} \quad (6)$$

Interval II ($\varepsilon \geq 0$):

$$\begin{cases} \dot{P}_{01} = W_{10}(P_{10} - P_{01}) + W_{11}^{\text{down}}(P_{11} - P_{01}) + W_{00}^{\text{up}}(P_{00} - P_{01}) + \Gamma P_{10} + \Gamma_R P_{00} + \Gamma_L P_{11} \\ \dot{P}_{10} = W_{11}^{\text{up}}(P_{11} - P_{10}) + W_{00}^{\text{down}}(P_{00} - P_{10}) + W_{10}(P_{01} - P_{10}) - \Gamma P_{10} + \Gamma_L P_{00} + \Gamma_R P_{11} \\ \dot{P}_{00} = W_{00}^{\text{down}}(P_{10} - P_{00}) + W_{00}^{\text{up}}(P_{01} - P_{00}) - \Gamma_R P_{00} - \Gamma_L P_{00} \\ P_{01} + P_{10} + P_{00} + P_{11} = 1 \end{cases} \quad (7)$$

For numerics, we used the following parameters: relaxation rates of the system are $\Gamma_1 = 0.9$ GHz, $\Gamma_R = 12$ GHz, $\Gamma_L = 50$ MHz, the energy splittings are equal to $\Delta_c = 8.25$ GHz, $\Delta_{\text{up}} = 1$ GHz, $\Delta_{\text{down}} = 21$ GHz, and their positions are at $\varepsilon = 0, \pm 255$ and ± 276 GHz respectively. The decoherence rate $\Gamma_2 = 4$ GHz and the excitation frequency $\nu = 4$ GHz.

By solving Eqs. (6, 7) for the stationary regime (when $dP_{ij}/dt = 0$), we obtain $P_{mn} = P_{mn}(\varepsilon_0, A)$, $m, n = 0, 1$ as a function of ε_0, A what allows us to plot the experimentally measured value, the quantum capacitance, which according to Ref. [28] can be written as

$$C = C_0 \frac{d}{d(\varepsilon_0)} \{P_{01} - P_{10} + a(P_{00} - P_{11})\}, \quad (8)$$

where a is a dimensionless factor which describes the DQD coupling to the fermionic sea, for the experiment $a = 18$ and C_0 is proportionality factor. The results of the theoretical calculations are presented in Fig. 2(a). The obtained interferogram shows the same patterns as the experimental one (see Fig. 3(b) in Ref. [28]). Specifically, one can see four different regimes: incoherent one (blue star), double-passage LZSM (green circle), single-passage LZSM (yellow triangle), multi-passage LZSM (red star). Fig. 2(b) presents a line cut of Fig. 2(a) at $A = 240$ GHz, the same patterns can be seen in the experiment (see Fig. 3(c) in Ref. [28]).

Figure 3 shows time dependence of probabilities for different regimes: (a) multi-passage LZSM; (b) single-passage LZSM; (c) incoherent one; (d) double-passage LZSM. From the plots one can conclude that the stationary regime (when $dP_{ij}/dt \approx 0$) starts after $t_0 \approx 0.8$ ns. Also it could be seen that for all cases $P_{01} > P_{10} > P_{11}, P_{00}$.

IV. THREE-LEVEL APPROXIMATION OF THE DQD

In this section we consider the system in the energy basis (in the previous section the system was described in the charge basis). In this case we can neglect the highest energy level ($P_3 = 0$) and take into account only three levels. Our energy level diagram has five avoided level crossings at $\varepsilon = 0, \pm\varepsilon_{21}^*$, and $\pm\varepsilon_{10}^*$. For the offsets from these points, we introduce $\varepsilon_{21}^\pm = \varepsilon \mp \varepsilon_{21}^*$ and $\varepsilon_{10}^\pm = \varepsilon \mp \varepsilon_{10}^*$, where \pm stand for $\varepsilon > 0$ and $\varepsilon < 0$. Respective rates are

$$W_c = \frac{\Delta_c^2}{2} \sum_n \frac{\Gamma_2 J_n^2 \left(\frac{A}{\nu} \right)}{(\varepsilon - n\nu)^2 + \Gamma_2^2}, \quad (9)$$

$$W_{21}^\pm = \frac{\Delta_{21}^2}{2} \sum_n \frac{\Gamma_{2,21} J_n^2 \left(\frac{A}{\nu} \right)}{(\varepsilon_{21}^\pm - n\nu)^2 + \Gamma_{2,21}^2}, \quad (10)$$

$$W_{10}^\pm = \frac{\Delta_{10}^2}{2} \sum_n \frac{\Gamma_{2,10} J_n^2 \left(\frac{A}{\nu} \right)}{(\varepsilon_{10}^\pm - n\nu)^2 + \Gamma_{2,10}^2}. \quad (11)$$

The rate equations (5) take the form

$$\begin{cases} \frac{dP_0}{dt} = [W_c + W_{10}^- + W_{10}^+] (P_1 - P_0) + \Gamma_{1 \rightarrow 0} P_1, \\ \frac{dP_1}{dt} = [W_c + W_{10}^- + W_{10}^+] (P_0 - P_1) + \\ \quad + [W_{21}^- + W_{21}^+] (P_2 - P_1) - \Gamma_{1 \rightarrow 0} P_1, \\ P_0 + P_1 + P_2 = 1. \end{cases} \quad (12)$$

These equations contain only leading terms; in particular, we omitted the term $\Gamma_{2 \rightarrow 0} P_2$ in the first equation and the term $\Gamma_{2 \rightarrow 1} P_2$ in the second equation. The fact that there is different relaxations between different levels is taken into account by assuming the time-dependent relaxation $\Gamma_{1 \rightarrow 0} = \Gamma_{1 \rightarrow 0}(t)$:

$$\Gamma_{1 \rightarrow 0}(t) = \begin{cases} \Gamma_1, & |\varepsilon(t)| < \varepsilon_{21}^*, \\ \Gamma_L, & |\varepsilon(t)| > \varepsilon_{21}^*, \end{cases} \quad (13)$$

where the first line describes the inter-dot relaxation, while the second line corresponds to the tunneling between the left dot and the leads.

Relation (13) provides two simplifications, when the whole dynamics is either for $|\varepsilon(t)| < \varepsilon_{21}^*$ or for $|\varepsilon(t)| > \varepsilon_{21}^*$. In these cases $\Gamma_{1 \rightarrow 0}$ becomes independent of time and we can have the stationary solution of the system of equations (12). (Then we can have the receipt for alike situations: take the analytical solutions for such regions, then fitting with this is a simple way to get the parameters; and afterwards one can continue with more elaborated calculations, such as solving time-dependent equations.) In these two particular cases we obtain analytical stationary solutions. For the coherent regime (“red-star” region) we have $W_{10}^\pm \rightarrow 0$ and $P_2 \rightarrow 0$, then it follows [32,49]

$$\begin{aligned} P_1 &= \frac{1}{2} \sum_{n=-\infty}^{\infty} \frac{\Delta_{c,n}^2}{\Delta_{c,n}^2 + \frac{\Gamma_1}{\Gamma_2} (\varepsilon_0 - n\nu)^2 + \Gamma_1 \Gamma_2}, \\ \Delta_{c,n} &= \Delta_c J_n \left(\frac{A}{\nu} \right). \end{aligned} \quad (14)$$

Analogously, for the incoherent regime (“blue-star” region) we have $W_c, W_{10}^- \rightarrow 0$ and $P_2 \rightarrow 0$, and then it follows

$$P_1 = \frac{1}{2} \sum_{n=-\infty}^{\infty} \frac{\Delta_{10,n}^2}{\Delta_{10,n}^2 + \frac{\Gamma_L}{\Gamma_{2,10}} (\varepsilon_{10}^+ - n\nu)^2 + \Gamma_L \Gamma_{2,10}}, \quad (15)$$

$$\Delta_{10,n} = \Delta_{10} J_n \left(\frac{A}{\nu} \right).$$

We can also note that in the lower parts of the $\varepsilon - A$ plane, below the red-star and the blue-star regions, all W 's are 0, and we have P_i all constants, resulting in zero C .

Otherwise, the time-dependent relaxation $\Gamma_{1 \rightarrow 0}(t)$ provides the dynamics during one driving period of two types "double-passage" and "incoherent" depending on do we reach one or two sides of the avoided-level crossings, at $\varepsilon_0 = \pm \varepsilon_{10}^*$. These considerations seem to justify that the system of equations above is sufficient for the whole picture.

V. CONCLUSIONS

We considered the rate-equation approach for a theoretical description of the four-level DQD. The system state as a function of the energy detuning ε and the amplitude of the excitation signal A was studied. We obtained that the DQD can be operated in four regimes in dependence on the considered parameters. These regimes are single-passage LZSM, which corresponds to small ε and large A ; double-passage LZSM (small A and ε); multi-passage LZSM (small A and ε); incoherent regime (large ε and small A). The research is important because it gives useful information about the DQD properties and behaviour which could be used for the system initializing and controlling.

Acknowledgments

S.N.S. acknowledges fruitful discussions with M.F. Gonzalez-Zalba. A.I.R. was supported by the RIKEN International Program Associates (IPA). This work was supported by Army Research Office (ARO) (Grant No. W911NF2010261).

Appendix A: Energy levels of a parallel double-quantum dot

In the current research we study the DQD proposed in Ref. [28], see Fig. 1(a). The first step in the system analysis is finding of the DQD energy levels. In the general form system electrostatic energy can be written:

$$E = \frac{1}{2} \vec{V} \cdot \mathbf{C} \vec{V} = \frac{1}{2} \vec{V} \cdot \vec{Q} = \frac{1}{2} \vec{Q} \cdot \mathbf{C}^{-1} \vec{Q}, \quad (A1)$$

where \vec{V} and \vec{Q} are the vectors of voltages and charges respectively, \mathbf{C} is the capacitance matrix. In Eq. (A1) we used $\vec{Q} = \mathbf{C} \vec{V}$. Thus to obtain the system energy levels we need to find the vector of charges and the inverse capacitance matrix of the system.

The charges $Q_{1,2}$ in the quantum dots can be written as follows

$$Q_1 = C_{T1}(V_1 - V_{TG}) + C_{B1}(V_1 - V_{BG}) + C_S(V_1 - V_S) + C_D(V_1 - V_D) + C_M(V_1 - V_2), \quad (A2)$$

$$Q_2 = C_{T2}(V_2 - V_{TG}) + C_{B2}(V_2 - V_{BG}) + C_S(V_2 - V_S) + C_D(V_2 - V_D) + C_M(V_2 - V_1). \quad (A3)$$

It is convenient to rewrite expressions (A2, A3) in a matrix form

$$\vec{Q} = \begin{pmatrix} Q_1 + C_{T1}V_{TG} + C_{B1}V_{BG} + C_S V_S + C_D V_D \\ Q_2 + C_{T2}V_{TG} + C_{B2}V_{BG} + C_S V_S + C_D V_D \end{pmatrix} = \begin{pmatrix} C_1 V_1 - C_M V_2 \\ C_2 V_2 - C_M V_1 \end{pmatrix}, \quad (A4)$$

where C_1 and C_2 are the capacitances, connected to the first and the second quantum dots respectively,

$$\begin{aligned} C_1 &= C_{T1} + C_{B1} + C_D + C_S + C_M, \\ C_2 &= C_{T2} + C_{B2} + C_D + C_S + C_M. \end{aligned} \quad (\text{A5})$$

Then the capacitance matrix has the following form:

$$\mathbf{C} = \begin{pmatrix} C_1 & -C_M \\ -C_M & C_2 \end{pmatrix}. \quad (\text{A6})$$

Let us assume for simplicity that $V_S = V_D = 0$. Then putting expressions for the vector of charges Eq. (A4) and for the inverse capacitance matrix Eq. (A6), for the DQD electrostatic energy we obtain:

$$\begin{aligned} E &= \frac{1}{C_1 C_2 - C_M^2} \left[\frac{1}{2} C_1 Q_2^2 + \frac{1}{2} C_2 Q_1^2 + C_M Q_1 Q_2 \right] + \frac{V_{TG}}{C_1 C_2 - C_M^2} [C_{T1} (C_M Q_2 + C_2 Q_1) + C_{T2} (C_1 Q_2 + C_M Q_1)] + \\ &\frac{V_{BG}}{C_1 C_2 - C_M^2} [C_{B1} (C_M Q_2 + C_2 Q_1) + C_{B2} (C_1 Q_2 + C_M Q_1)] + \frac{V_{TG}^2}{C_1 C_2 - C_M^2} \left[\frac{1}{2} C_1 C_{T2}^2 + \frac{1}{2} C_2 C_{T1}^2 + C_{T1} C_{T2} C_M \right] + \\ &\frac{V_{BG}^2}{C_1 C_2 - C_M^2} \left[\frac{1}{2} C_1 C_{T2}^2 + \frac{1}{2} C_2 C_{T1}^2 + C_{T1} C_{T2} C_M \right]. \end{aligned} \quad (\text{A7})$$

In order to simplify Eq. (A7), let us introduce new values, $N_i = -\frac{Q_i}{|e|}$, for the number of electrons in the i th quantum dot, and reduced top-gate n_t and back-gate n_b voltages

$$n_t = \frac{C_{T1} V_{TG}}{|e|} = \frac{1}{1+a} \frac{C_{T2} V_{TG}}{|e|}, \quad (\text{A8})$$

$$n_b = \frac{C_{B1} V_{BG}}{|e|} = \frac{1}{1-a} \frac{C_{B2} V_{BG}}{|e|}, \quad (\text{A9})$$

where a is an asymmetry factor in the gate couplings. Assuming $C = C_1 = C_2 = m C_M$ and rewriting the quantum dot charges as $Q_{1(2)} = -|e| N_{1(2)}$, then for the energy of the quantum dot we have:

$$\begin{aligned} \frac{E}{E_C} &= \frac{1}{2} N_1^2 + \frac{1}{2} N_2^2 + \frac{N_1 N_2}{m} - n_t \left[N_1 + \frac{N_2}{m} + (1+a) \left(N_2 + \frac{N_1}{m} \right) \right] \\ &- n_b \left[N_1 + \frac{N_2}{m} + (1-a) \left(N_2 + \frac{N_1}{m} \right) \right] + n_t^2 \left[\frac{1}{2} + \frac{1}{2} (1+a)^2 + \frac{1+a}{m} \right] \\ &+ n_b^2 \left[\frac{1}{2} + \frac{1}{2} (1-a)^2 + \frac{1-a}{m} \right] + n_t n_b \left[2 \left(1 + \frac{1}{m} \right) - a^2 \right], \end{aligned} \quad (\text{A10})$$

where we defined $E_C = E_{C_1} = E_{C_2} = m E_{C_M} = e^2 \frac{C}{C^2 - C_M^2}$. We plot the energy levels diagram in Fig. 1(b) for the following parameters: $a = 0.1$, $n_b = 0.25$, $m = 10$, and $(N_1, N_2) = (0, 1)$.

* e-mail: liul@ilt.kharkov.ua

- ¹ M. Veldhorst, J. C. C. Hwang, C. H. Yang, A. W. Leenstra, B. de Ronde, J. P. Dehollain, J. T. Muhonen, F. E. Hudson, K. M. Itoh, A. Morello, and A. S. Dzurak, "An addressable quantum dot qubit with fault-tolerant control-fidelity," *Nat. Nanotechnol.* **9**, 981–985 (2014).
- ² M. D. Shulman, O. E. Dial, S. P. Harvey, H. Bluhm, V. Umansky, and A. Yacoby, "Demonstration of entanglement of electrostatically coupled singlet-triplet qubits," *Science* **336**, 202–205 (2012).
- ³ J. R. Petta, A. C. Johnson, J. M. Taylor, E. A. Laird, A. Yacoby, M. D. Lukin, C. M. Marcus, M. P. Hanson, and A. C. Gossard, "Coherent manipulation of coupled electron spins in semiconductor quantum dots," *Science* **309**, 2180–2184 (2005).
- ⁴ R. Hanson, L. H. W. van Beveren, I. T. Vink, J. M. Elzerman, W. J. M. Naber, F. H. L. Koppens, L. P. Kouwenhoven, and L. M. K. Vandersypen, "Single-shot readout of electron spin states in a quantum dot using spin-dependent tunnel rates," *Phys. Rev. Lett.* **94**, 196802 (2005).

- ⁵ H. Kiyama, T. Nakajima, S. Teraoka, A. Oiwa, and S. Tarucha, “Single-shot ternary readout of two-electron spin states in a quantum dot using spin filtering by quantum hall edge states,” *Phys. Rev. Lett.* **117**, 236802 (2016).
- ⁶ M. Friesen, C. Tahan, R. Joynt, and M. A. Eriksson, “Spin readout and initialization in a semiconductor quantum dot,” *Phys. Rev. Lett.* **92**, 037901 (2004).
- ⁷ V. Cerletti, W. A. Coish, O. Gywat, and D. Loss, “Recipes for spin-based quantum computing,” *Nanotechnology* **16**, R27 (2005).
- ⁸ D. Loss and D. P. DiVincenzo, “Quantum computation with quantum dots,” *Phys. Rev. A* **57**, 120–126 (1998).
- ⁹ D. P. DiVincenzo, D. Bacon, J. Kempe, G. Burkard, and K. B. Whaley, “Universal quantum computation with the exchange interaction,” *Nature* **408**, 339–342 (2000).
- ¹⁰ M. S. Byrd and D. A. Lidar, “Comprehensive encoding and decoupling solution to problems of decoherence and design in solid-state quantum computing,” *Phys. Rev. Lett.* **89**, 047901 (2002).
- ¹¹ K. Kim, “Visible light emissions and single-electron tunneling from silicon quantum dots embedded in Si-rich SiO₂ deposited in plasma phase,” *Phys. Rev. B* **57**, 13072–13076 (1998).
- ¹² M. J. Romero and J. van de Lagemaat, “Luminescence of quantum dots by coupling with nonradiative surface plasmon modes in a scanning tunneling microscope,” *Phys. Rev. B* **80**, 115432 (2009).
- ¹³ J. C. Estrada Saldaña, A. Vekris, G. Steffensen, R. Žitko, P. Krogstrup, J. Paaske, K. Grove-Rasmussen, and J. Nygård, “Supercurrent in a double quantum dot,” *Phys. Rev. Lett.* **121**, 257701 (2018).
- ¹⁴ S. Sasaki, S. Amaha, N. Asakawa, M. Eto, and S. Tarucha, “Enhanced Kondo effect via tuned orbital degeneracy in a spin 1/2 artificial atom,” *Phys. Rev. Lett.* **93**, 017205 (2004).
- ¹⁵ C. W. J. Beenakker and A. A. M. Staring, “Theory of the thermopower of a quantum dot,” *Phys. Rev. B* **46**, 9667–9676 (1992).
- ¹⁶ C. Simon, Y.-M. Niquet, X. Caillet, J. Eymery, J.-P. Poizat, and J.-M. Gérard, “Quantum communication with quantum dot spins,” *Phys. Rev. B* **75**, 081302 (2007).
- ¹⁷ J. Huwer, R. M. Stevenson, J. Skiba-Szymanska, M. B. Ward, A. J. Shields, M. Felle, I. Farrer, D. A. Ritchie, and R. V. Pentyl, “Quantum-dot-based telecommunication-wavelength quantum relay,” *Phys. Rev. Appl.* **8**, 024007 (2017).
- ¹⁸ R. M. Abolfath, A. G. Petukhov, and I. Žutić, “Piezomagnetic quantum dots,” *Phys. Rev. Lett.* **101**, 207202 (2008).
- ¹⁹ H. Flentje, P.-A. Mortemousque, R. Thalineau, A. Ludwig, A. D. Wieck, C. Bauerle, and T. Meunier, “Coherent long-distance displacement of individual electron spins,” *Nat. Commun.* **8** (2017).
- ²⁰ T. Brandes, “Coherent and collective quantum optical effects in mesoscopic systems,” *Phys. Rep.* **408**, 315–474 (2005).
- ²¹ W. G. van der Wiel, S. De Franceschi, J. M. Elzerman, T. Fujisawa, S. Tarucha, and L. P. Kouwenhoven, “Electron transport through double quantum dots,” *Rev. Mod. Phys.* **75**, 1–22 (2002).
- ²² D. Awschalom and M. Flatte, “Challenges for semiconductor spintronics,” *Nature Phys.* **3**, 153 (2007).
- ²³ S. Donsa, S. Andergassen, and K. Held, “Double quantum dot as a minimal thermoelectric generator,” *Phys. Rev. B* **89**, 125103 (2014).
- ²⁴ R. Aguado and L. P. Kouwenhoven, “Double quantum dots as detectors of high-frequency quantum noise in mesoscopic conductors,” *Phys. Rev. Lett.* **84**, 1986–1989 (2000).
- ²⁵ T. Liu, Q.-P. Su, J.-H. Yang, Y. Zhang, S.-J. Xiong, J.-M. Liu, and C.-P. Yang, “Transferring arbitrary d-dimensional quantum states of a superconducting transmon qubit in circuit QED,” *Sci. Rep.* **7** (2017).
- ²⁶ Y. Wang, Z. Hu, B. C. Sanders, and S. Kais, “Qudits and high-dimensional quantum computing,” *Front. Phys.* **8** (2020).
- ²⁷ Y. Han, X.-Q. Luo, T.-F. Li, W. Zhang, S.-P. Wang, J. Tsai, F. Nori, and J. You, “Time-domain grating with a periodically driven qutrit,” *Phys. Rev. Appl.* **11**, 014053 (2019).
- ²⁸ A. Chatterjee, S. N. Shevchenko, S. Barraud, R. M. Otxoa, F. Nori, J. J. L. Morton, and M. F. Gonzalez-Zalba, “A silicon-based single-electron interferometer coupled to a fermionic sea,” *Phys. Rev. B* **97**, 045405 (2018).
- ²⁹ A. Ferrón, D. Domínguez, and M. J. Sánchez, “Tailoring population inversion in Landau-Zener-Stückelberg interferometry of flux qubits,” *Phys. Rev. Lett.* **109**, 237005 (2012).
- ³⁰ A. Ferrón, D. Domínguez, and M. J. Sánchez, “Dynamic transition in Landau-Zener-Stückelberg interferometry of dissipative systems: The case of the flux qubit,” *Phys. Rev. B* **93**, 064521 (2016).
- ³¹ M. P. Liul and S. N. Shevchenko, “Rate-equation approach for multi-level quantum systems,” *Low Temp. Phys.* **49**, 102–108 (2023).
- ³² D. M. Berns, W. D. Oliver, S. O. Valenzuela, A. V. Shytov, K. K. Berggren, L. S. Levitov, and T. P. Orlando, “Coherent quasiclassical dynamics of a persistent current qubit,” *Phys. Rev. Lett.* **97**, 150502 (2006).
- ³³ W. D. Oliver and S. O. Valenzuela, “Large-amplitude driving of a superconducting artificial atom,” *Quantum Inf. Process.* **8**, 261–281 (2009).
- ³⁴ X. Wen and Y. Yu, “Landau-Zener interference in multilevel superconducting flux qubits driven by large-amplitude fields,” *Phys. Rev. B* **79** (2009).
- ³⁵ A. Izmalkov, M. Grajcar, E. Il’ichev, N. Oukhanski, T. Wagner, H.-G. Meyer, W. Krech, M. H. S. Amin, A. M. van den Brink, and A. M. Zagorskin, “Observation of macroscopic Landau-Zener transitions in a superconducting device,” *Europhys. Lett.* **65**, 844–849 (2004).
- ³⁶ M. A. Nakonechnyi, D. S. Karpov, A. N. Omelyanchouk, and S. N. Shevchenko, “Multi-signal spectroscopy of qubit-resonator systems,” *Low Temp. Phys.* **37**, 383 (2021).
- ³⁷ C. H. Chien, M. P. Liul, C. Y. Chen, P. Y. Wen, J. C. Chen, Y. H. Lin, S. N. Shevchenko, F. Nori, and I. C. Hoi, “Coherent dynamics of a photon-dressed qubit,” (2022).
- ³⁸ G. Fuchs, G. Burkard, P. Klimov, and D. Awschalom, “A quantum memory intrinsic to single nitrogen-vacancy centres in diamond,” *Nature Phys.* **7**, 789–793 (2011).

- ³⁹ H. Ribeiro and G. Burkard, “Nuclear state preparation via Landau-Zener-Stückelberg transitions in double quantum dots,” *Phys. Rev. Lett.* **102**, 216802 (2009).
- ⁴⁰ A. Thiel, “The Landau-Zener effect in nuclear molecules,” *J. Phys. G: Nucl. Part. Phys.* **16**, 867–910 (1990).
- ⁴¹ L. Zhu, A. Widom, and P. M. Champion, “A multidimensional Landau-Zener description of chemical reaction dynamics and vibrational coherence,” *J. Chem. Phys.* **107**, 2859–2871 (1997).
- ⁴² D. Bouwmeester, N. H. Dekker, F. E. v. Dorselaer, C. A. Schrama, P. M. Visser, and J. P. Woerdman, “Observation of Landau-Zener dynamics in classical optical systems,” *Phys. Rev. A* **51**, 646–654 (1995).
- ⁴³ J. Stehlik, Y. Dovzhenko, J. R. Petta, J. R. Johansson, F. Nori, H. Lu, and A. C. Gossard, “Landau-Zener-Stückelberg interferometry of a single electron charge qubit,” *Phys. Rev. B* **86**, 121303 (2012).
- ⁴⁴ W. D. Oliver, Y. Yu, J. C. Lee, K. K. Berggren, L. S. Levitov, and T. P. Orlando, “Mach-Zehnder interferometry in a strongly driven superconducting qubit,” *Science* **310**, 1653–1657 (2005).
- ⁴⁵ M. F. Gonzalez-Zalba, S. N. Shevchenko, S. Barraud, J. R. Johansson, A. J. Ferguson, F. Nori, and A. C. Betz, “Gate-sensing coherent charge oscillations in a silicon field-effect transistor,” *Nano Lett.* **16**, 1614–1619 (2016).
- ⁴⁶ P. O. Kofman, O. V. Ivakhnenko, S. N. Shevchenko, and F. Nori, “Majorana’s approach to nonadiabatic transitions validates the adiabatic-impulse approximation,” *Sci. Rep.* **13**, 5053 (2023).
- ⁴⁷ K. Ono, S. N. Shevchenko, T. Mori, S. Moriyama, and F. Nori, “Quantum interferometry with a g -factor-tunable spin qubit,” *Phys. Rev. Lett.* **122**, 207703 (2019).
- ⁴⁸ T. Wu, Y. Zhou, Y. Xu, S. Liu, and J. Li, “Landau-Zener-Stückelberg interference in nonlinear regime,” *Chin. Phys. Lett.* **36**, 124204 (2019).
- ⁴⁹ O. V. Ivakhnenko, S. N. Shevchenko, and F. Nori, “Nonadiabatic Landau-Zener-Stückelberg-Majorana transitions, dynamics and interference,” *Phys. Rep.* **995**, 1–89 (2023).
- ⁵⁰ Y. Nakamura and J. S. Tsai, “A coherent two-level system in a superconducting single-electron transistor observed through photon-assisted cooper-pair tunneling,” *J. Supercond.* **12**, 799–806 (1999).
- ⁵¹ M. S. Rudner, A. V. Shytov, L. S. Levitov, D. M. Berns, W. D. Oliver, S. O. Valenzuela, and T. P. Orlando, “Quantum phase tomography of a strongly driven qubit,” *Phys. Rev. Lett.* **101**, 190502 (2008).
- ⁵² R. K. Malla and M. Raikh, “Landau-Zener transition between two levels coupled to continuum,” *Phys. Lett. A* **445**, 128249 (2022).
- ⁵³ J.-D. Chen, X.-D. Wen, G.-Z. Sun, and Y. Yu, “Landau-Zener-Stückelberg interference in a multi-anticrossing system,” *Chin. Phys. B* **20**, 088501 (2011).
- ⁵⁴ Y. Wang, S. Cong, X. Wen, C. Pan, G. Sun, J. Chen, L. Kang, W. Xu, Y. Yu, and P. Wu, “Quantum interference induced by multiple Landau-Zener transitions in a strongly driven rf-squid qubit,” *Phys. Rev. B* **81**, 144505 (2010).
- ⁵⁵ X. Wen, Y. Wang, S. Cong, G. Sun, J. Chen, L. Kang, W. Xu, Y. Yu, P. Wu, and S. Han, “Landau-Zener-Stuckelberg interferometry in multilevel superconducting flux qubit,” *arXiv* (2010).
- ⁵⁶ R. M. Otxoa, A. Chatterjee, S. N. Shevchenko, S. Barraud, F. Nori, and M. F. Gonzalez-Zalba, “Quantum interference capacitor based on double-passage Landau-Zener-Stückelberg-Majorana interferometry,” *Phys. Rev. B* **100**, 205425 (2019).
- ⁵⁷ J. He, D. Pan, M. Liu, Z. Lyu, Z. Jia, G. Yang, S. Zhu, G. Liu, J. Shen, S. N. Shevchenko, F. Nori, J. Zhao, L. Lu, and F. Qu, “Quantifying quantum coherence of multiple-charge states in tunable josephson junctions,” *arXiv* (2023).